CAD Models for Shielded Multilayered CPW

Spartak Gevorgian, L. J. Peter Linnér, *Senior Member, IEEE,* and Erik L. Kollberg, *Fellow, IEEE*

***Abstract*—Conformal mapping technique is used to obtain CAD oriented closed form analytical expressions for characteristic impedance per unit length capacitance and relative effective dielectric permittivity of top and bottom shielded multilayered coplanar waveguides. Analytical expressions are deduced for a wide verity of CPW structures.**

I. Introduction

RECENT PROGRESS in High Temperature Superconductor (HTSC) Microwave Devices [1], [2], Integrated Optical Traveling-Wave Modulators (TWM) [3], [4] and optically controlled microwave devices [5] has initiated an extensive study of Coplanar Waveguides (CPW). In Microwave Integrated Circuits (MIC) CPW have complex structure [6], [7] in contrast with that first proposed by Wen [8]. In packaged MIC's metal walls are introduced above and below the CPW. Full-wave analysis is usually used to characterize such complex CPW structures [9]–[11]. These analysis provide high precision in a wide frequency band. On the other hand conformal mapping techniques lead to closed form analytical solutions [12] suitable for CAD software packages and they provide a simulation accuracy comparable with full-wave techniques [13] for frequencies up to 20 GHz. Furthermore, analytical expressions have been derived for coupled CPW [14], microwave losses in metal strips [15], [16] and multilayered dielectric substrates of CPW [17]. This emphasizes the potential of conformal mapping techniques.

In this paper the conformal mapping method is applied to derive analytical approximations for basic characteristics of top and bottom shielded multilayered CPW. The method is based on extension of the partial capacitance technique originally proposed by Veyers and Hanna [18]. Although not rigorously valid for complex waveguiding structures it provides reasonable accuracy and is used extensively for CPW [19] and coplanar-strip waveguides [20]. For practical characteristic impedances the transverse dimensions are small compared to the wavelength and the slots in CPW are modeled as magnetic walls. Moreover, losses in metal strips and dielectric layers are assumed to be small so that quasi-TEM approximation could be applied. Additionally, "low frequencies" allow us to neglect the effect of longitudinal fields introduced due to the condition $\varepsilon_1, \varepsilon_2 \neq \varepsilon_3$ or ε_4. Two basic shielded CPW models are studied (Fig. 1). In this paper $\varepsilon_3 = \varepsilon_4 = 1$ is assumed for the sake of simplicity. In general ε_3 and ε_4 may have any reasonable value which slightly changes the expressions of the effective dielectric permittivities of the lines.

Manuscript received April 4, 1994; revised July 25, 1994.

The authors are with the Chalmers University of Technology, S-412 96 Göoteborg, Sweden.

IEEE Log Number 9408560.

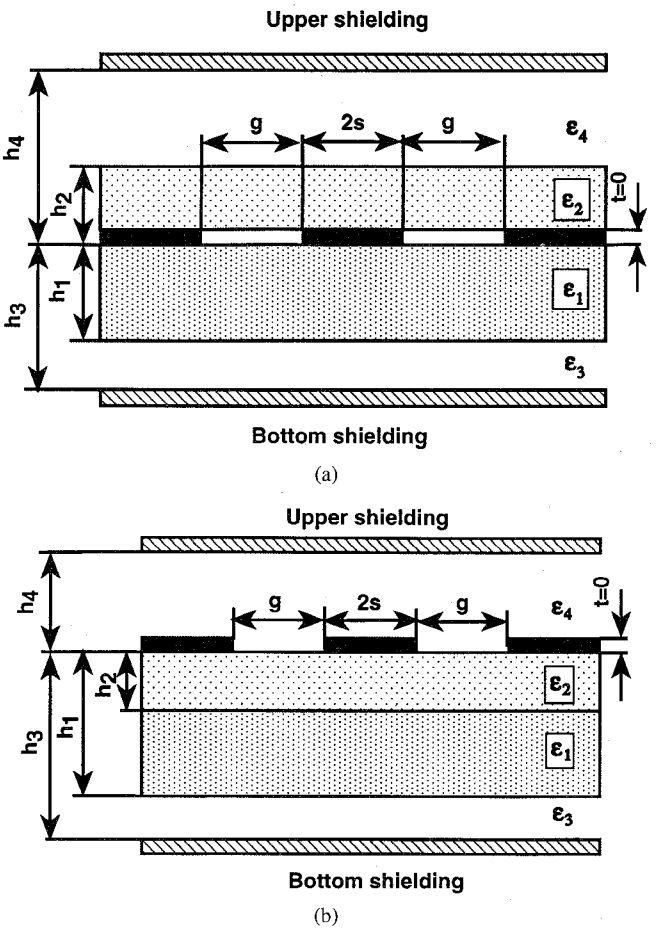

Fig. 1. (a) Two-layered substrate and (b) dielectric coated shielded CPW's.

II. Analysis

A. Conformal Transformations

In the quasi-TEM limit the basic characteristics of CPW, the wave impedance and the propagation constant are given when the capacitance per unit length is known. The capacitances per unit length of the waveguiding structures under study are determined assuming zero thickness of metal strips. The line capacitance of CPW is presented as a sum of partial capacitances. For the dielectric loaded CPW, Fig. 1(a), the partial capacitances are determined from structures illustrated in Fig. 2(a)–(d). As mentioned above the layers next to shieldings are assumed to be air filled, $\varepsilon_3 = \varepsilon_4 = 1$. Fig. 2(a) and (c) present air-filled spaces below and above the

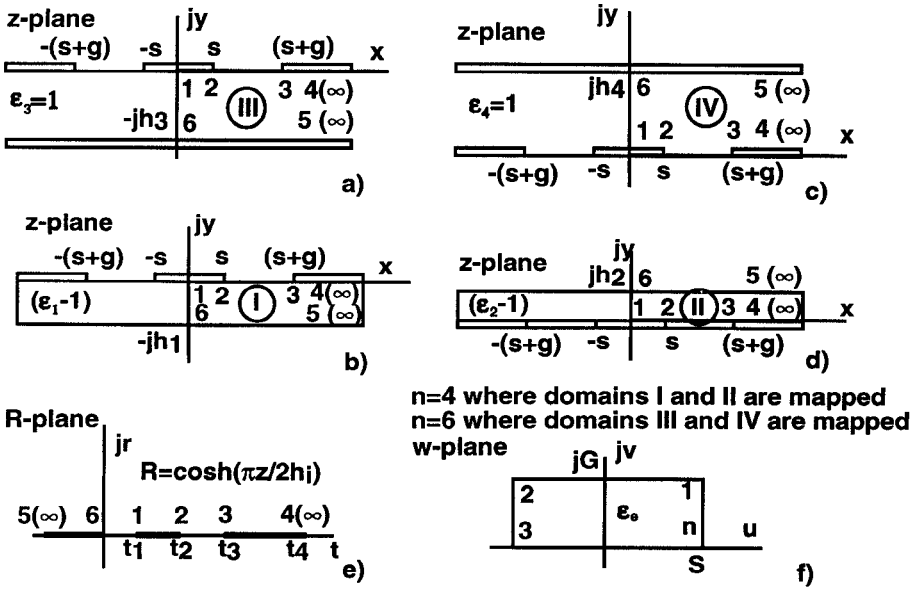

Fig. 2. Conformal transformations for evaluation of partial capacitances.

metal strips of CPW in the absence of dielectric layers. Partial capacitances due to these spaces are denoted by C_{03} and C_{04}. The other partial capacitances are due to a substrate with equivalent relative permittivity $(\varepsilon_1 - 1)$, Fig. 2(b), and dielectric load with equivalent relative dielectric permittivity $(\varepsilon_2 - 1)$, Fig. 2(d). These capacitances are denoted by C_1 and C_2. For determination of the partial capacitances we use conformal mapping technique by mapping all domains of z-plane in Fig. 2(a)–(d) onto the internal domain of the same rectangular in w-plane, Fig. 2(f). Air-dielectric [12], [16]–[20] and dielectric to dielectric interfaces are modeled as magnetic walls. As far as the mapped regions are symmetric only right-hand halves of Fig. 2(a)–(d) have to be considered. The conformal transformation is performed in two steps. First the function

$$t = \cosh^2\left(\frac{\pi z}{2h_i}\right), \quad i = 1, 2, 3, 4 \tag{1}$$

is used to map the domains I–IV of Fig. 2(a)–(d) onto the upper half of Fig. 2(e). The thicknesses h_i in (1) are shown in Figs. 1 and 2. Below the same notations are used for two-layered substrate CPW, Fig. 1(b). These notations lead to simple and similar expressions for the CPW studied in this paper. The mappings of the domains I to IV of Fig. 2(a)–(d) onto the R-plane by using (1) result in the following coordinates:

$$t_1 = 1; \quad t_2 = \cosh^2\left(\frac{\pi s}{2h_i}\right); \quad t_3 = \cosh^2\left(\frac{\pi(s+g)}{2h_i}\right). \tag{2}$$

The second conformal mapping transforms the domains of the upper half of the R-plane, Fig. 2(e), to the internal domain of rectangle in w-plane, Fig. 2(f), using Christoffel–Schwartz transformation. In the case of the domains III and IV, Fig. 2(a) and (c), we arrive to the following function:

$$W = \frac{2A_1}{\sqrt{(t_3 - t_1)t_2}} F(\varphi, k) + A_2 \tag{3}$$

where $F(\varphi, k)$ is an elliptic integral of the first kind with

$$\varphi = \operatorname{arin}\sqrt{\frac{(t - t_3)t_2}{(t - t_2)t_3}} \tag{4}$$

$$k = \sqrt{\frac{t_3(t_2 - t)}{(t_3 - 1)t_2}}. \tag{5}$$

The constants A_1 and A_2 are determined from correspondence of vertices in t- and w-planes using (2)–(5) and Fig. 2(a) and (f).

In the case where the domains I and II, Fig. 2(b) and (d), are concerned with the application of Christoffel–Schwartz transformation leads to the following function:

$$W = \frac{2B_1}{\sqrt{t_3 - t_1}} F(\varphi, k) + B_2 \tag{6}$$

with

$$\varphi = \operatorname{arin}\sqrt{\frac{t_3 - 1}{t - 1}} \tag{7}$$

$$k = \sqrt{\frac{t_2 - 1}{t_3 - 1}}. \tag{8}$$

As before, the constants B_1 and B_2 are determined from boundary conditions using (2) and (6)–(8).

The above functions map all "partial" regions of CPW, Fig. 2(a)–(d) onto the same internal region of a rectangular in w-plane, Fig. 2(f). Thus these mappings are equivalent to connection in parallel the partial capacitances of CPW to form a resultant parallel-plate capacitor of Fig. 2(f) with a capacitance $C = C_{04} + C_{03} + C_2 + C_1$

$$C = \varepsilon_0 \varepsilon_e \frac{2S}{G}. \tag{9}$$

The relative effective dielectric permittivity ε_e and the ratio $2S/G$ are determined below.

B. Dielectric Loaded CPW (Fig. 1(a))

The partial capacitance introduced by air filled region III, Fig. 2(a), with $h_i = h_3$ is easily found by substituting t_2 and t_3 from (2) into the (3)–(5) and applying boundary conditions to Fig. 2(e) and (f). The result of this transformation is

$$C_{03} = \varepsilon_0 \frac{K(k_3)}{K(k_3')} \tag{10}$$

where the modulus of the complete elliptic integrals $K(k_3)$ and $K(k_3')$ are given by

$$k_3 = \frac{\tanh\left(\frac{\pi s}{2h_3}\right)}{\tanh\left[\frac{\pi(s+g)}{2h_3}\right]}. \tag{11}$$

$k_3' = \sqrt{1-k_3^2}$. A similar procedure gives

$$C_{04} = \varepsilon_0 \frac{K(k_4)}{K(k_4')} \tag{12}$$

with $k_4' = \sqrt{1-k_3^2}$, and

$$k_4 = \frac{\tanh\left(\frac{\pi s}{2h_4}\right)}{(\tanh)\left[\frac{\pi(s+g)}{2h_4}\right]}. \tag{13}$$

For calculation of the partial capacitance due to the substrate, Fig. 2(b), with thickness $h_i = h_1$ and equivalent relative dielectric permittivity $(\varepsilon_1 - 1)$ we use (2) along with (6) and Fig. 2(e) and (f). The result is

$$C_1 = (\varepsilon_1 - 1)\varepsilon_0 \frac{K(k_1)}{K(k_1')} \tag{14}$$

$k_1' = \sqrt{1-k_1^2}$,

$$k_1 = \frac{\sinh\left(\frac{\pi s}{2h_1}\right)}{(\sinh)\left[\frac{\pi(s+g)}{2h_1}\right]}. \tag{15}$$

For a dielectric load of thickness $h_i = h_4$, Fig. 2(d), and the equivalent relative dielectric permittivity $(\varepsilon_2 - 1)$ from (2), (6)–(8) one can derive

$$C_2 = (\varepsilon_2 - 1)\varepsilon_0 \frac{K(k_2)}{K(k_2')} \tag{16}$$

with $k_2' = \sqrt{1-k_2^2}$,

$$k_2 = \frac{\sinh\left(\frac{\pi s}{2h_2}\right)}{\sinh\left[\frac{\pi(s+g)}{2h_2}\right]}. \tag{17}$$

According to (9), the total capacitance is $C = 2(C_{04} + C_{03} + C_2 + C_1)$

$$C = 2\varepsilon_0\varepsilon_e \left[\frac{K(k_3)}{K(k_3')} + \frac{K(k_4)}{K(k_4')}\right]. \tag{18}$$

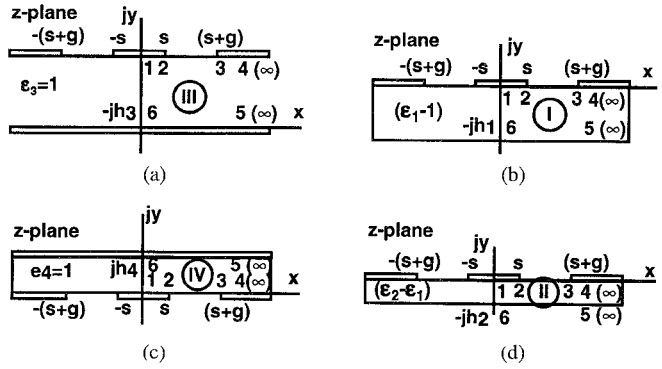

Fig. 3. Conformal transformations for two-layered substrate CPW.

The coefficient 2 in (18) is due to the left-hand sides of Fig. 2(a)–(d). In (18) the effective dielectric permittivity of the line determined as

$$\varepsilon_e = 1 + q_1(\varepsilon_1 - 1) + q_2(\varepsilon_2 - 1) \tag{19}$$

where the partial filling factors are given by

$$q_1 = \frac{K(k_1)}{K(k_1')}\left[\frac{K(k_3)}{K(k_3')} + \frac{K(k_4)}{K(k_4')}\right] \tag{20}$$

$$q_2 = \frac{K(k_2)}{K(k_2')}\left[\frac{K(k_3)}{K(k_3')} + \frac{K(k_4)}{K(k_4')}\right]. \tag{21}$$

The characteristic impedance of the CPW is now

$$Z_0 = \frac{60\pi}{\sqrt{\varepsilon_e}}\left[\frac{K(k_3)}{K(k_3')} + \frac{K(k_4)}{K(k_4')}\right]^{-1}. \tag{22}$$

C. Two-Layered Substrate CPW (Fig. 1(b))

The thickness of the substrate is $(h_1 - h_2)$, Fig. 1(b), and the relative dielectric permittivity ε_1. The thickness and the dielectric permittivity of the superstrate are h_2 and ε_2. As in the previous case the capacitance per unit length is derived as a sum of partial capacitances determined from Fig. 3. Keeping the same notations for this CPW we arrive to expressions (10) and (12) for the partial capacitances of lower and upper domains given by Fig. 3(a) and (c).

Now, assuming the equivalent relative dielectric permittivity of the substrate $(\varepsilon_1 - 1)$ we map the area I, Fig. 3(b), onto the t-plane, Fig. 2(e), by using the transformation (1). The procedure used for the previous case leads to the partial capacitance given by (14). The partial capacitance introduced by a layer of thickness h_2 and equivalent permittivity $(\varepsilon_2 - \varepsilon_1)$ is obtained by mapping the area II, Fig. 3(d), on the same internal domain of w-plane, Fig. 2(f), by the sequence of transformations given by functions (1) and (6). The resulting partial capacitance is

$$C_2 = (\varepsilon_2 - \varepsilon_1)\varepsilon_0 \frac{K(k_2)}{K(k_2')}. \tag{24}$$

The modulus of the elliptic integrals are given by (17). Now combining (10), (12), (14), and (24) the line capacitance of

two-layered substrate CPW can be given as

$$C = 2\varepsilon_0\varepsilon_e\left[\frac{K(k_3)}{K(k_3')} + \frac{K(k_4)}{K(k_4')}\right] \tag{25}$$

where the effective dielectric permittivity is determined by

$$\varepsilon_e = 1 + q_1(\varepsilon_1 - 1) + q_2(\varepsilon_2 - \varepsilon_1) \tag{26}$$

with filling factors given by (20) and (21). In this case for line impedance we have

$$Z_0 = \frac{60\pi}{\sqrt{\varepsilon_e}}\left[\frac{K(k_3)}{K(k_3')} + \frac{K(k_4)}{K(k_4')}\right]^{-1}. \tag{27}$$

III. Limiting Cases

In this section we discuss some limiting cases to confirm the validity of the above analysis. Also it will be shown that analytical expressions could be deduced for a wide verity of CPW structures.

A. Dielectric Loaded Unshielded CPW

For unshielded CPW in Fig. 1 and (11) and (13) $h_3 = h_4 = \infty$ leading to $k_3 = k_4 = k_0$, where

$$k_0 = \frac{s}{s+g} \tag{28}$$

with $K(k_3) = K(k_4) = K(k_0)$ and

$$q_1 = \frac{1}{2}\frac{K(k_1)}{K(k_1')}\frac{K(k_0')}{K(k_0)}; \quad q_2 = \frac{1}{2}\frac{K(k_2)}{K(k_2')}\frac{K(k_0')}{K(k_0)} \tag{29}$$

as follows from (21) and (22). The effective dielectric permittivity is obtained from (19) by substituting filling factors from (29). The capacitance per unit length and the characteristic impedance are deduced from (18) and (22)

$$C = 4\varepsilon_0\varepsilon_e\frac{K(k_0)}{K(k_0')} \tag{30}$$

$$Z_0 = \frac{30\pi}{\sqrt{\varepsilon_e}}\frac{K(k_0')}{K(k_0)}. \tag{31}$$

For $h_2 = 0$ limit from (17) we have $k_2 = 0$ and from (29) $q_2 = 0$. This reduces the dielectric permittivity from (19) to

$$\varepsilon_e = 1 + \frac{\varepsilon_1 - 1}{2}\frac{K(k_1)}{K(k_1')}\frac{K(k_0')}{K(k_0)} \tag{32}$$

a result first given by Veyers and Hanna [18]. From (19) for $\varepsilon_2 = 1$ limit we are left with (32) at any h_2 value. In addition for $h_1 = \infty$ limit $k_1 = k_0$ and from (32) one can get the well-known approximation first given by Wen [8]

$$\varepsilon_e = \frac{1+\varepsilon_1}{2}. \tag{33}$$

B. Two-Layered Unshielded CPW

For this CPW the assumption $h_3 = h_4 = \infty$ leads to (28) and (29). Then the effective permittivity is determined substituting (29) into (26). For this new effective permittivity the line capacitance and impedance are determined from (30) and (31).

Now if the thickness of the dielectric layer $h_2 = 0$, Figs. 1(b) and 3, from (17) we find $k_2 = 0$, which means that $K(k_2)/K(k_2') = 0$ and $q_2 = 0$. For this case from (26) we arrive to (32). From (26) we arrive to the same well known permittivity, (32), for any value of h_2 where $\varepsilon_1 = \varepsilon_2$. Additionally from (26) follows (33). Further, for $h_2 = \infty$ limit ($h_2 < h_1$) we have an infinitely thick substrate CPW with relative dielectric permittivity ε_2 and effective dielectric permittivity $(\varepsilon_2 + 1)/2$.

C. Conductor Backed CPW with Upper Shielding

For both the CPW's studied, Fig. 1, the $h_2 = h_3$ limit should be discussed specially since at this limit one has a rapid change in the boundary conditions and the expression for k_1 in, (15), becomes invalid. In this case the application of (7) for mapping of regions I and III in Figs. 2 and 3 onto the internal region of rectangle in the w-plane, Fig. 2(f), is not valid and the function (3) should be used instead. The bottom shielding serves as an additional ground plane. Implementation of (3) to regions I in Figs. 2 and 3 leads to complete elliptic integrals $K(k_{11})$ and $K(k_{11}')$ with modulus $k_{11}' = \sqrt{1-k_{11}^2}$ and

$$k_{11} = \frac{\tanh\left(\frac{\pi s}{2h_1}\right)}{\tanh\left[\frac{\pi(s+g)}{2h_1}\right]}. \tag{15'}$$

Hence for both types of conductor backed CPW the results of above the analysis are applicable provided that instead k_1, (15), k_{11} is used.

For the dielectric loaded CPW, Fig. 1(a), at $h_2 = h_4$ limit instead of k_2 given by (17), the following expression should be used:

$$k_{22} = \frac{\tanh\left(\frac{\pi s}{2h_2}\right)}{\tanh\left[\frac{\pi(s+g)}{2h_2}\right]}. \tag{17'}$$

On the other hand for thick substrates where the arguments of sinh and tanh functions are small for conductor backed CPW (15) and (17) still can be used. For $h_1 < g$ limit, special care should be taken where the air gap, $(h_3 - h_1)$, between substrate and bottom shielding is small and comparable with the field "penetration depth" beyond the bottom surface of the substrate. For $h_1 < g$ limit, the analysis of Section II is applicable with high accuracy if $(h_3 - h_1) > \lambda_0[2\pi\sqrt{\varepsilon_e - 1}]^{-1}$, where λ_0 is the free space wavelength. It should be noted that the main limitations regarding h_4, h_2, and ε_2 discussed above are also applicable to the conductor backed CPW with the exception $h_4 = 0$ for dielectric loaded waveguide, Fig. 1(a). A summary of limiting CPW structures is given in Appendix A.

IV. Numerical Results

Although the validity of the expressions derived in Section II have been proven in some special cases in the previous section here we provide additional comparison of the results

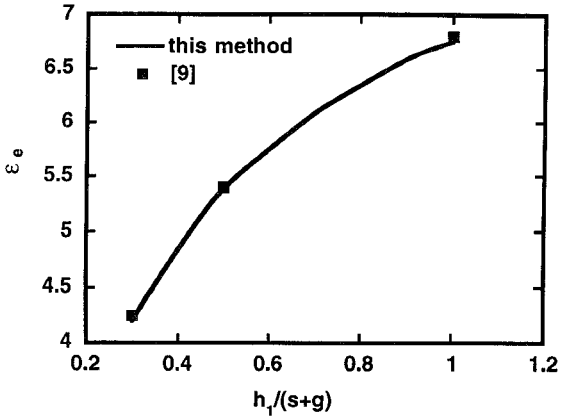

Fig. 4. The effective dielectric permittivity of unshielded dielectric-coated CPW.

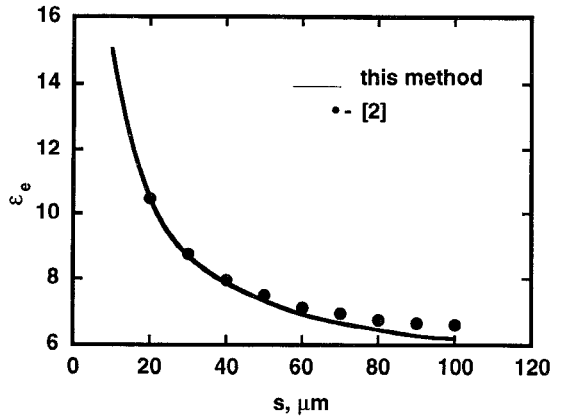

Fig. 5. The effective dielectric permittivity of unshielded two-layered substrate CPW.

TABLE I
THE WAVE IMPEDANCE OF TWO-LAYERED SUBSTRATE CPW

2s, μm	g, μm	Z_o, Ohm		
		measured [4]	calculated [4]	this method
20	5	27	25 7-27.1	24 80-25 48
48	10	24 5	24 1-25 0	22.98-23 32
150	25	23	21 9-22.4	21 28-21-40

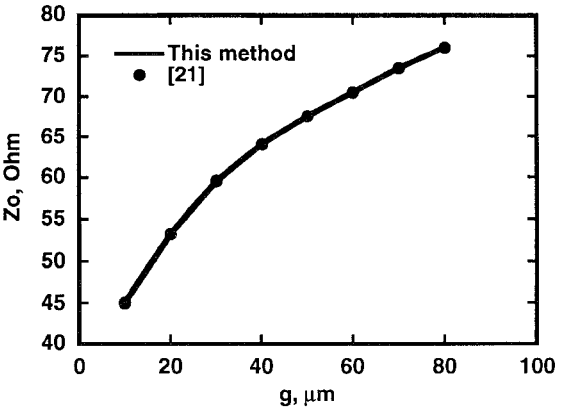

Fig. 6. The wave impedance of unshielded two-layered CPW.

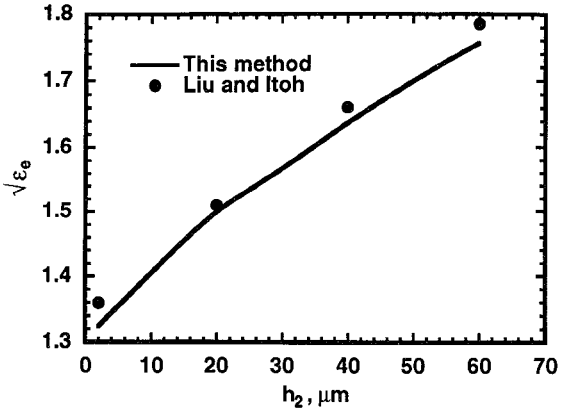

(a)

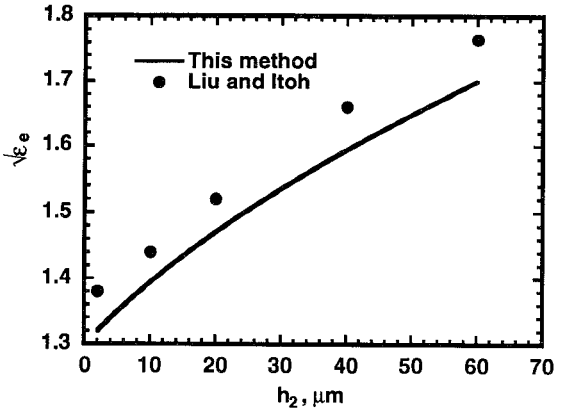

(b)

Fig. 7. The effective dielectric permittivities of conductor-backed shielded CPW. (a) Dielectric-loaded CPW. (b) Two-layered substrate CPW.

of the analysis with results of available full-wave analysis and experiments. The dependence of the effective dielectric permittivity for unshielded dielectric loaded CPW is given in Fig. 4. In computations $h_3 = h_4 = \infty$ is assumed with $h_1 = 750$ mm, $h_2 = 150$ μm, ε_1, ε_2. The data are taken from [9] where the computations has been carried out using spectral-domain approach. As it follows from Fig. 4, the agreement between two results is within 1.5%. In Fig. 5, the dependence the effective dielectric permittivity of two layered substrate CPW upon gapwidth g is compared with the results of partial wave analysis [2]. In this case the following data have been used in computations: $\varepsilon_1 = 10$, $\varepsilon_2 = 1500$, $h_2 = 0.1$ μm, $h_1 = h_3 = h_4 = \infty$, $s/g = 1$. It follows from Fig. 5 that the ε_e from [2] is slightly larger. The discrepancy perhaps is due to the kinetic inductance of superconductor films used in [2]. Experimental data for wave impedance of two-layered substrate CPW could be found in [4]. A comparison of calculated characteristic impedance obtained in this work with experimental and theoretical results of [4] contains the Table I.

The data used in the calculations $\varepsilon_1 = \sqrt{(28.3 \bullet 43)}$, $\varepsilon_2 = 2.14$, $h_2 = 0.6 \div 0.85$ μm, $h_1 = 1000$ μm. Excellent agreement has been found for wave impedance of two layered CPW experimentally studied by Patterson [21]. Fig. 6 shows

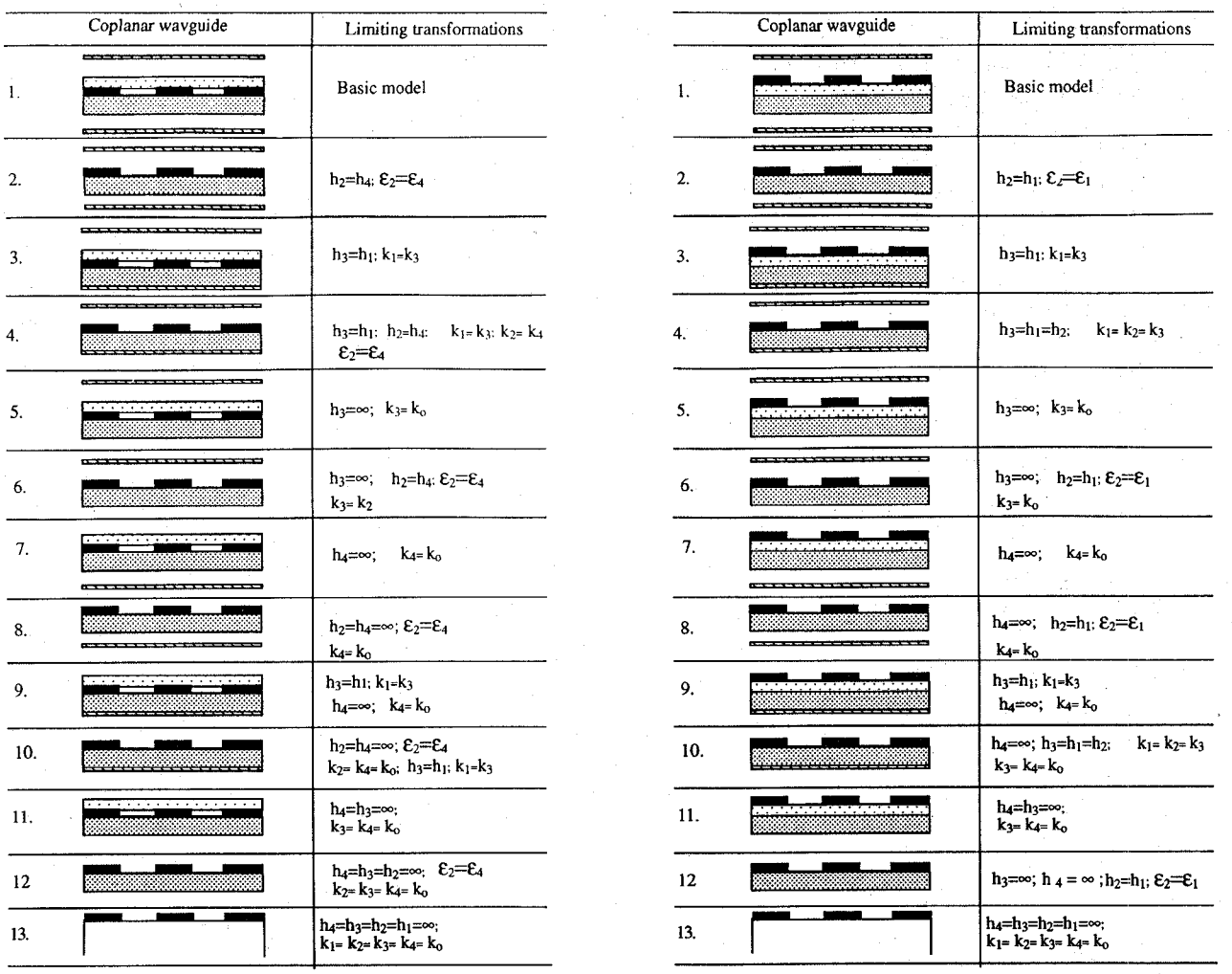

Fig. 8. Appendix A: (a) Limiting structures for dielectric coated shielded CPW model. (b) Limiting structures for two-layered shielded coplanar waveguide model.

the dependence of Z_0 upon half-gap width g with experimental point and data taken from [21]. The CPW consists of 2.2-μm-thick alternating silicon nitride/oxide layers laid on top of 635-μm-thick gallium arsenide substrate.

Computation for a conductor backed CPW without upper shielding have been carried out for the model given in [10]. In this model $\varepsilon_1 = 13$, $h_2 = 0$, $h_1 = h_3$, $2s = 200$ μm, $g = 100$ μm. The results of these computations are presented in Table II indicating good agreement. The dependencies of effective dielectric permittivity of shielded conductor backed dielectric loaded and two-layered substrate CPW are shown in Fig. 7. The results of full-wave analysis are for 10 GHz from Liu and Itoh [22].

Computations for top and bottom shielded CPW, Fig. 1(a), with $h_1 = 1000$ μm, $h_2 = 0$, $\varepsilon_1 = 9.35$, $h_3 = 5500$ μm, $2s = g = 2000$ μm have been compared with the results of spectral-domain analysis [11]. The large divergence in ε_e (6%) could be attributed to poor accuracy of quasistatic model for large g limits.

For computation of the ratio of the elliptic integrals well known approximations [12] can be used for k and k' values

TABLE II
SLOWING FACTORS FOR CONDUCTOR-BACKED CPW

h_1, μm	$1/\varepsilon_e$,this method	$1/\varepsilon_e$,[10]
50	0.316	0.319
100	0.339	0.339
150	0.359	0.352
300	0.383	0.368
500	0.393	0.374

in the range $0.1 \div 0.9$. Determination of line parameters for $h_i \to 0$ limit faces some computational problems concerned the accuracy and singularities at in k and k' near the 0 and 1. Approximations given in Appendix B are aimed to overcome this problem.

V. CONCLUSION

The characteristic impedance and the effective dielectric permittivity of CPW's calculated using the method presented above are in good agreement with the experimental and

theoretical results available in the literature. The validity and the accuracy of the expressions are within the limits well known for conformal mapping based quasi-TEM approximations used for CPW. Although $\varepsilon_3 = \varepsilon_4 = 1$ have been assumed in this work the expressions for ε_e can be written for general $\varepsilon_3 \neq \varepsilon_4 \neq 1$ case making the expressions slightly complex. Also the models can be extended for CPW with more dielectric layers than has been used in this work. From general expressions obtained for multilayered shielded CPW's analytical approximations are deduced for a wide verity of practical CPW structures. The analytical expressions are general and highly suitable to be used in complex CAD packages. Their accuracy can be improved using the method described in [13].

APPENXIX A (See Fig. 8, above)

APPENDIX B

1) Approximations for the elliptic integrals ratio. An efficient and fast converging ratio for the complete elliptic integrals of the first kind can be derived from q-series [23]. Assuming $m = k^2$ and $m_1 = 1 - k^2$ we write

$$\frac{K(k)}{K(k')} = -\pi\left\{\ln\left[\frac{m}{16} + 8\left(\frac{m}{16}\right)^2 + 84\left(\frac{m}{16}\right)^3 + 992\left(\frac{m}{16}\right)^4 + \cdots\right]\right\}^{-1}, \quad \text{for} \quad 0 < k \leq 1/\sqrt{2} \tag{B1}$$

and

$$\frac{K(k)}{K(k')} = -\frac{1}{\pi}\left\{\ln\left[\frac{m_1}{16} + 8\left(\frac{m_1}{16}\right)^2 + 84\left(\frac{m_1}{16}\right)^3 + 992\left(\frac{m_1}{16}\right)^4 + \cdots\right]\right\}, \quad \text{for} \quad 1 > k \geq 1/\sqrt{2}. \tag{B2}$$

The computation accuracy is better than 10^{-8}.

2) Approximations for $h_2 = 0$ limit. For this limit from (17) we have

$$k_2 \approx \exp\left(-\frac{\pi g}{2h_2}\right).$$

For $k = 0$ $(m = 0)$ limit in (B1) taking only the first term we get

$$\frac{K(k_2)}{K(k_2')} \approx \frac{h_2}{g}.$$

REFERENCES

[1] N. Newman and G. W. Lyons, "High-temperature superconducting microwave devices: Fundamental issues in materials, physics and engineering," *J. Supercond.*, vol. 6, no. 3, pp. 119–160, 1993.

[2] J. Keßler, R. Dill, and P. Russer, "Influence of buffer layers within YBCO coplanar waveguide structures," *IEEE Microwave and Guided Wave Lett.*, vol. 2, Jan. 1992.

[3] O. G. Ramer, "Integrated optics electrooptic modulator electrode analysis," *J. Quantum Electron.*, vol. 18, pp. 386–392, Mar. 1982.

[4] H. Chung, W. S. C. Chang, and G. E. Bettes, "Microwave properties of travelling-wave electrodes in $LiNbO_3$ electrooptic modulators," *J. Lightwave Technol.*, vol. 11, pp. 1274–1278, Aug. 1993.

[5] Special issue on "Application of lightwave technology to microwave devices, circuits and systems,"*IEEE Trans. Microwave Theory Tech.*, vol. 38, May 1990.

[6] T. Itoh, Ed., *Numerical Technique for Microwave and Millimeter-Wave Passive Circuits*. New York: Wiley, 1989.

[7] M. S. Soghomonian and I. D. Robertson, "Finite difference modeling of novel waveguiding structures for MMIC applications," *Int. J. Microwave Millimeter-Wave Comp. Aided Eng.*, vol. 3, pp. 271–286, 1993.

[8] C. P. Wen, "Coplanar waveguide: A surface strip transmissiom line suitable for nonreciprocal gyrometric device applications," *IEEE Trans. Microwave Theory Tech.*, vol. 17, pp. 1087–1090, Dec. 1969.

[9] C.-N. Chang, W.-C. Chang, and C. H. Chen, "Full-wave analysis of multilayer coplanar lines," *IEEE Trans. Microwave Theory Tech.*, vol. 39, pp. 747–750, Apr. 1991.

[10] K. K. M. Cheng and J. K. A. Everard, "A new technique for the quasi-TEM analysis of conductor backed coplanar structures," *IEEE Trans. Microwave Theory Tech.*, vol. 41, pp. 1589–1592, Sept. 1993.

[11] M. R. Lyons, J. P. K. Gilb, and C. A. Balanis, "Enhanced domain mode operation of a shielded multilayer coplanar waveguide via substrate compression," *IEEE Trans. Microwave Theory Tech.*, vol. 41, pp. 1589–1592, Sept. 1993.

[12] R. Schinzinger and P. A. A. Laura, *Conformal Mapping: Methods and Applications*. Amsterdam, The Netherlands: Elselvier, 1991.

[13] S. S. Bedair and I. Wolf, "Fast, accurate and simple approximate analytic formulas for calculating the parameters of supported coplanar waveguides for (M)MIC's," *IEEE Trans. Microwave Theory Tech.*, vol. 40, pp. 41–48, Jan. 1992.

[14] V. F. Hanna, "Parameters of coplanar directional couplers with lower ground plane," in *Proc. 15th Eur. Microwave Conf.*, 1985, pp. 820–825.

[15] L. J. P. Linnér, "A method for the computation of the characteristic immitance matrix of multiconductor striplines with arbitrary widths," *IEEE Trans. Microwave Theory Tech.*, vol. 22, pp. 930–937, Nov. 1974.

[16] G. Ghione, "A CAD oriented analytical model for the losses of general asymmetric coplanar lines in hybrid and monolithic MIC's," *IEEE Trans. Microwave Theory Tech.*, vol. 41, Sept. 1993.

[17] S. S. Gevorgian, D. I. Kaparkov, and O. G. Vendik, "Electrically controlled HTSC/ferroelectric coplanar waveguide," *Inst. Elect. Eng. Proc.*, pt. H, vol. 141, pp. 501–503, 1994.

[18] C. Veyers and V. F. Hanna, "Extention of the application of conformal mapping techniques to coplanar lines with finite dimentions," *Int. J. Electron.*, vol. 48, pp. 47–56, Jan. 1980.

[19] G. Ghione and C. Naldi, "Coplanar waveguides for MMIC applications; Effects of upper shielding, conductor backing, finite-extent ground +planes, and line-to-line coupling," *IEEE Trans. Microwave Theory Tech.*, vol. 35, pp. 260–267, Mar. 1987.

[20] S. S. Gevorgian and I. G. Mironenko, "Asymmetric coplanar-strip transmission lines for MMIC and integrated optics applications," *Electron. Lett.*, vol. 26, no 22, pp. 1516–1517, 1990.

[21] H. Patterson, "Modeling lossy transmission lines from S-parameter data," *Microwave J.*, pp. 96–104, Nov. 1993.

[22] Y. Lui and T. Itoh, "Leakage phenomena in multilayered conductor backed coplanar waveguides," *IEEE Microwave and Guided Wave Lett.*, vol. 3, pp. 426–427, 1993.

[23] M. Abramowitz and I. A. Stegun, *Handbook of Mathematical Functions*. New York: Dover, 1970.

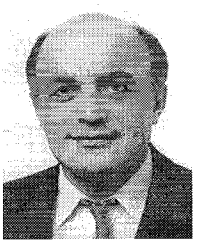

Spartak Gevorgian graduated in electronic engineering in 1972 from Engineering University of Armenia, Yerevan, and received the Ph.D. and Doctor of Sciences degrees from Leningrad Electrical Engineering University, St. Petersburg, Russia, in 1977 and 1991, respectively.

From 1977 to 1988, he was with the Engineering University of Armenia as a reader (docent), and from 1991 to 1993, as a full professor. Since September 1993, he has been a professor in the Electrical Engineering University of St. Petersburg, Russia. His fields of interest are in microwave integrated circuits, integrated optics, and optically controlled microwave devices. He is presently engaged in the development of HTSC-based microwave devices at the Department of Microwave Technology, Chalmers University of Technology, Sweden. He is the author of the monograph, "Glass Based Integrated Optical Devices" (St. Petersburg, Russia) and more than 70 scientific papers in Russian and international publications.

L. J. Peter Linnér (S'98–M'74–SM'87) received the M.Sc. and Ph.D. degrees in electrical engineering from Chalmers University of Technology, Gothenburg, Sweden, in 1969 and 1974, respectively.

Since 1969, he has been a teaching assistant in mathematics and telecommunications at Chalmers University of Technology. In 1973, he became a member of the research and teaching staff of the Division of Network Theory at the same university with research interests in the areas of network theory, microwave engineering, and computer-aided design methods. In 1974, he joined the MI-division, Ericsson Telephone Company, MIndal, Sweden, where he was a systems engineer and project leader in several military radar projects. He returned to Chalmers University of Technology as a researcher in the areas of microwave array antenna systems. Since 1981 he has been a university lecturer in telecommunications. For part of 1992, he spent a period at University of Bochum, Germany, as a guest researcher. His current interest is in the application of computer-aided network methods in the area of microwave and antenna technology.

Erik L. Kollberg (M'83–SM'83–F'91), received his Teknologie Doktor degree in 1970 from Chalmers University of Technology, Goteborg, Sweden in 1974

Following an associate professorship, he became Professor at the Electrical Engineering Department of Chalmers 1979. He was on a six months sabbatical leave to Caltech, Pasadena until March 1991. Most of his work has been focused on low noise receiver technology for applications in radio astronomy at Onsala Space Observatory, and he has published more than 150 papers. From 1963 to 1976 he conducted research on low-noise maser amplifiers. Various types of masers were developed for the frequency range of 1–35 GHz. In 1972 he initiated research on low-noise millimeter wave Schottky diode mixers, and in 1981 on millimeter and submillimeter wave superconducting quasiparticle mixers. Recently he has broadened his interest in high Tc superconducting circuits and semiconductor devices, including various kinds of diodes and three- terminal devices.

Dr. Kollberg won the 1982 Microwave Prize at the 12th European Microwave Conference in Helsinki, Finland. He was awarded the Gustaf Dahlén gold medal in 1986.